

~~CONFIDENTIAL~~Copy 194
RM L52H08

NACA RM L52H08

TECH LIBRARY KAFB, NM
0144440

NACA

RESEARCH MEMORANDUM

A STUDY OF THE ZERO-LIFT DRAG-RISE CHARACTERISTICS OF
WING-BODY COMBINATIONS NEAR THE SPEED OF SOUND

By Richard T. Whitcomb

Langley Aeronautical Laboratory
Langley Field, Va.Classification cancelled (or changed to *Unclassified*)By Authority of *NASA Tech Rep Announcement #92*
(OFFICER AUTHORIZED TO CHANGE)By *27 Sep 55*
NAME ANDGRADE OF OFFICER MAKING CHANGE)
*10 Apr 61*This material contains information affecting the National Defense of the United States within the meaning
of the espionage laws, Title 18, U.S.C., Sec. 793 and 794, and the transmission or the revelation of its
contents in any manner to an unauthorized person is prohibited by law.NATIONAL ADVISORY COMMITTEE
FOR AERONAUTICS

WASHINGTON

September 3, 1952

~~CONFIDENTIAL~~*279. 5/10**1118163*



NATIONAL ADVISORY COMMITTEE FOR AERONAUTICS

RESEARCH MEMORANDUM

A STUDY OF THE ZERO-LIFT DRAG-RISE CHARACTERISTICS OF
WING-BODY COMBINATIONS NEAR THE SPEED OF SOUND

By Richard T. Whitcomb

SUMMARY

Comparisons have been made of the shock phenomena and drag-rise increments for representative wing and central-body combinations with those for bodies of revolution having the same axial distributions of cross-sectional area normal to the air stream. On the basis of these comparisons, it is concluded that near the speed of sound the zero-lift drag-rise of a thin low-aspect-ratio wing-body combination is primarily dependent on the axial distribution of the cross-sectional areas normal to the air stream. It follows that the drag rise for any such configuration is approximately the same as that for any other with the same distribution of cross-sectional areas.

Investigations have also been made of representative wing-body combinations with the body so indented that the axial distributions of cross-sectional areas for the combinations were the same as that for the original body alone. Such indentations greatly reduced or eliminated the zero-lift drag-rise increments associated with the wings near the speed of sound.

INTRODUCTION

In the interpretation of the zero-lift drag-rise characteristics of configurations near the speed of sound, the transonic similarity rules and linear theory have been applied in limited analyses. However, no general means is available for directly explaining quantitatively the variations of the transonic drag rise associated with the numerous changes in wing plan form and section considered by airplane designers (ref. 1, for example), even for the simplified case of a wing alone. More important, even a qualitative understanding of the large and highly variable zero-lift drag interferences associated with practical combinations of wings and bodies near the speed of sound (refs. 2, 3, and 4, for example) has been lacking. A logical means for interpreting

the drag-rise values for thin low-aspect-ratio wing-body configurations is discussed herein.

The results presented in reference 5 indicate that for a representative swept-wing and central-body combination, the zero-lift drag rise is due primarily to shock losses. A study of these results also indicates that the shock formations about this relatively complex configuration at zero lift near the speed of sound are similar to those that would be expected for a body of revolution with the same axial distribution of cross-sectional area normal to the air stream. (The probable shocks for such a body were estimated on the basis of the flow surveys presented in ref. 6.) Further, the drag-rise characteristics for this wing-body combination at zero lift are about the same as those for a body of revolution (ref. 7) with approximately the same axial distribution of cross-sectional area. On the basis of these facts and a preliminary consideration of the general physical nature of the flow about configurations, it has been reasoned that near the speed of sound the zero-lift drag rise of a wing-body configuration generally should be primarily dependent on the axial distribution of the cross-sectional areas normal to the air stream.

In order to ascertain the soundness of this concept, measurements have been made of the flow fields and drag-rise characteristics for four representative wing-central-body combinations and for bodies of revolution with the same axial distributions of cross-sectional area normal to the air stream. The results, obtained at Mach numbers from 0.85 to 1.10 in the Langley 8-foot transonic tunnel, are compared and analyzed herein. In order to illustrate possibilities for improving airplane performance at transonic speeds, zero-lift drag coefficients for three special wing-body combinations are also presented.

EXPERIMENTS

Configurations

Basic bodies.— The major part of the results discussed herein were obtained for three wings in conjunction with the body of revolution shown in figures 1(a), 1(b), and 1(c). The body is normally cylindrical in the region of the wing and has a forebody of the same shape as that of the body described in reference 5. The radii of the cylindrical body are listed in table I. The swept wing of the group was also investigated in conjunction with the body with a curved afterbody as shown in figure 1(d). This combination is identical with that of reference 5. Radii of the curved body are also listed in table I. The maximum diameter of this curved body is somewhat less than that of the cylindrical body.

Wings.— The wing for which the most extensive results were obtained has 0° sweep of the quarter-chord line, an aspect ratio of 4.0, and a taper ratio of 0. The streamwise sections of the wing are symmetrical, 4 percent thick, and consist of circular arcs with the maximum thickness at the 40-percent-chord stations. This configuration (fig. 1(a)) is referred to as the "unswept" wing. Results were also obtained with this wing reversed so that the 75 percent chord line is unswept, as shown in figure 1(b). The leading-edge sweep of this wing is 37° . This configuration is very nearly of delta plan form and is referred to as the "delta" wing. Finally, investigations were made with a wing which has 45° sweep of the quarter-chord line, an aspect ratio of 4.0, a taper ratio of 0.6, and an NACA 65A006 airfoil section parallel to the air stream. This configuration (figs. 1(c) and 1(d)) is referred to as the "swept" wing.

Special bodies.— Bodies of revolution with the same axial distributions of cross section as the wing-body combinations were obtained by altering the original bodies. The radii of these revised bodies of revolution are listed in table II. Especially indented bodies of revolution were investigated in conjunction with the three wings and these bodies were also obtained by altering the original cylindrical body. The radii of these bodies in the region of the wing are listed in table III.

Measurements

Schlieren surveys were obtained with the temporary schlieren system described in reference 6. In order to obtain side-view schlieren surveys of the fields at distances from the model center lines with the horizontal, symmetrically oriented schlieren system, the various models were displaced downward from the center line of the tunnel, as shown in figure 2(a). In every case the displacement for the comparable bodies of revolution were the same as for the wing-body combination. Plan-view schlieren surveys for the unswept-wing--body configuration were obtained by rotating the model 90° and displacing it farther from the center line of the tunnel. Wall Mach number distributions were obtained from pressures measured at the rows of orifices placed along the center lines of panels of the test section adjacent to the top and bottom panels as shown in figure 2(a). The relative radial locations of the wall Mach number measurement stations with respect to the model are indicated in figure 2(a). For the side-view schlieren surveys the distances from the model center lines to these stations were 35.5 and 52.8 inches. For the plan-view surveys, they were 31.2 and 58.0 inches. Drag measurements were obtained by internal strain-gage balances. Base pressures were also measured.

Presentation of Results

Detailed flow surveys.- Composites of the schlieren photographs and wall Mach number M_w distributions for the unswept wing and cylindrical body combination, the comparable body of revolution, and the cylindrical body alone are presented in figure 2 for several stream Mach numbers M_o . The schlieren photographs shown above the center lines of the outlines of the three configurations present side views; those below the center line of the wing-body configuration present plan views. The plan-view schlieren surveys for the wing-body configurations were not duplicated for the bodies of revolution. The relative orientations and sizes of the photographs with respect to the outlines are the same as those of the schlieren fields with respect to the test model. (See sketches in fig. 2(a)).

The wall Mach number distributions shown at the tops of the composites for the three configurations were obtained during side-view schlieren surveys, those at the bottoms of the composites for the wing-body combination are from plan-view surveys (see sketches in fig. 2(a)). The two Mach number distributions presented on a given set of ordinates are for the two measurement stations, designated with the corresponding symbols in the sketches in figure 2(a). The Mach number distributions are placed on the composites so that the distances from the center line of the model to the M_o points on the Mach number scales are equal relatively to the distances from the model to the lower-wall Mach number measurement stations, as indicated by the circle symbol in the sketch in figure 2(a). The horizontal scale of the wall Mach number distributions is the same as that for the model outline.

The stream Mach numbers M_o at which the various schlieren pictures and wall Mach number distributions were obtained varied by as much as ± 0.005 from the mean values for each of the composites. However, the maximum difference between the stream Mach number for the directly comparable side-view photographs for the wing-body combination and the comparable body of revolution was approximately 0.003.

Drag coefficients.- The zero-lift drag coefficients C_{D_o} for the wing-body combinations, the comparable bodies of revolution, and the basic bodies alone, as presented in the various figures such as figure 3, are all based on wing areas of 1 square foot. These coefficients have been corrected to a condition at which the base pressure is equal to the stream static pressure. The drag coefficient increments ΔC_{D_o} , as presented in figure 3, have been obtained by subtracting the drag coefficient values measured at a Mach number of approximately 0.85 from those measured at the higher Mach numbers. This subtraction nearly eliminated the effects of differences in the skin friction of the

comparable configurations on the comparisons of the drag characteristics for these configurations.

The maximum error of the absolute drag coefficients presented is approximately ± 0.0005 . The effects of wall-reflected disturbances, as described in reference 6, on the drag results have been essentially eliminated at all Mach numbers except those near a value of about 1.05. This has been accomplished by displacing the model from the tunnel center line (ref. 6), using a cylindrical afterbody on the larger body, and correcting for the base pressure variations. No results were obtained for Mach numbers near 1.05.

Schlieren photographs.— The schlieren fields for the delta and swept wings, (fig. 4, for example) were oriented with respect to the configurations as indicated by the lowest schlieren photographs and configuration outlines.

DISCUSSION

In the discussion that follows the basic comparisons and analyses are made for the unswept-wing—cylindrical-body combination. The results for the other combinations indicate the effects of several variations of the wing and body configurations on the phenomena.

Unswept Wing and Cylindrical Body

Shock phenomena.— The wall Mach number distributions and schlieren photographs presented in figures 2(a) to 2(d) indicate that the extensive shock formations produced by the unswept-wing—cylindrical-body combination at the test Mach numbers near the speed of sound are almost exactly the same as those caused by the body of revolution with the same axial distribution of cross-sectional area, except in the local region directly downstream of the wing. In this locality, the shock formations, while not as closely similar as at greater distances from the configurations, are at least approximately comparable. (The incompatible shock crossing the downstream, plan-view schlieren photograph, at a Mach number of 1.03 is a weak reflection of a disturbance of the configuration from the tunnel wall.) At a Mach number of 1.10 (fig. 2(e)), the similarities of the schlieren photographs for the comparable configurations are less close than at Mach numbers near 1.0.

A study of the physical nature of the flow indicates that the similarities of the extensive shock formations produced by the wing-body combination and a body of revolution with the same axial distribution of cross-sectional area near the speed of sound can logically be attributed

primarily to two basic factors: the negligible variations of stream-tube areas with changes in velocity (ref. 8) and the concentration of the effects of a disturbance in a plane nearly normal to the air stream. (These two factors are basically related.) It is apparent that because of the second factor, the streamwise locations of the effects of the disturbances of the wing should be essentially the same as those for the corresponding effects produced by the body of revolution with the same axial distribution of disturbances. Also because of the second factor, the analysis of the lateral similarities of the fields of the comparable configurations may be greatly simplified by considering the flow changes in each normal plane independently.

As a starting point for the analysis of the lateral similarities, consider the flow about the comparable configurations in a given normal plane at a circle, concentric to the axis of symmetry, outside the tip of the wing. As a result of the essential invariance of the stream tubes, the total radial deviations of the fields at this circle are essentially the same as the displacements of the surfaces of the configurations in the same plane. Since the total surface displacements for the two configurations are the same, the total flow deviations at the circle must be essentially equal. However, circumferential variations of these deviations may exist for the wing-body configuration. The essential irrotationality of the flow leads to reductions of these circumferential variations with increase in distance from the configuration. Because of the invariance of the stream-tube areas, these reductions are relatively rapid. This invariance causes the outer field to be relatively inflexible. As a result, it reacts strongly to the circumferential variations of the radial deviations, producing pronounced circumferential pressure gradients. These gradients cause deviations in the circumferential direction which markedly reduce the variations of the radial deviations. Such effects lead to an essential elimination of the circumferential variations of radial deviations at a relatively short distance from the configuration. Also, any initial circumferential deviations associated with the asymmetry of the wing-body combination are rapidly dissipated with increase in radial distance. As a consequence of the rapid dissipation of both the circumferential deviations and the variations of radial deviations with radial distance, the deviations in a given plane at a short distance from the wing-body configuration are nearly the same as the axially symmetric effects produced by the comparable body of revolution. Such agreements for the various normal planes result in the observed similarities of the strong shock formations for the wing-body combination and the comparable body of revolution at a distance from the configurations.

The strong reactions of the flow in the outer regions of the field of the wing-fuselage combination to deviations from axial symmetry, as described above, converge toward the axis of symmetry and reduce the asymmetrical deviations, even in the immediate region of the wing.

These reactions force the inner field into at least an approximate similarity to the axially symmetric field of the body of revolution with the same axial distribution of disturbances, as shown in figure 2.

As the Mach number is increased to supersonic values, the fields of the various disturbances become conical. Also, at these speeds, changes in velocities result in variations of the stream-tube areas. Consequently, the similarities of the shock formations for the wing-body combination and the comparable body of revolution should be progressively lessened as the Mach number is increased beyond the speed of sound.

Drag characteristics.- The close similarity of the shock formations for the wing-body combination and the body of revolution with the same axial variation of cross-sectional area in most regions of the fields suggests that in these regions the energy losses associated with the shocks for the two configurations should be nearly the same. In the locality directly downstream of the wing, the shock losses for the two configurations may differ somewhat; however, the relative effect of such differences should be unimportant. Because of the invariance of the stream-tube areas near a Mach number of 1.0, the fields of flow for these, or any configuration, are relatively extensive. As a result, the greater part of the shock losses for the configurations is due to the large areas of significantly strong shock outside the local region downstream of the wing. Thus, the differences between the shock losses for the wing-body combination and the comparable body in the local region near the wing should result in relatively small differences of the total losses for the two configurations. Also, because of the low thickness ratio and aspect ratio of the wing and the gradual curvature for the comparable body, the shock-induced separation losses for these configurations should be relatively small, although probably not negligible, and any differences of these losses should be small. Therefore, the drag rise for the combination should be approximately the same as that for the comparable body of revolution.

The measured increments of drag coefficient for the unswept wing-body combination are the same as those for the comparable body of revolution within the probable accuracy of the data (fig. 3). (The absolute drag coefficients for the comparable configurations differ somewhat, primarily because of differences in skin friction.)

The exact agreement of the drag-rise increments for the unswept wing-body combination with those for the comparable body of revolution suggests that the secondary separation losses, as well as the primary shock losses, are essentially the same for the two configurations. This apparent agreement can logically be attributed to the fact that the relationships between the shocks and boundary layers for the wing-body combination and the comparable bodies are roughly the same.

The similarity of the drag-rise values for the comparable configurations at a Mach number of 1.10 indicates that the perceptible deviations of the shock formations for the two configurations noted at this Mach number (fig. 2(e)) result in insignificant differences of the shock losses.

Delta Wing and Cylindrical Body

Shock phenomena.- Wall Mach number distributions indicate that, as for the unswept-wing-body combination, the flow fields for the delta-wing-body combination at a distance from the configuration are generally almost exactly the same as those for the body of revolution with the same axial distribution of cross-sectional area for all test Mach numbers. The schlieren photographs presented in figure 4 indicate that in the field above the aft part of the wing, the shocks for the wing-body combination are approximately the same as those for the comparable body. As for the unswept-wing-body combination, the most pronounced deviations of the shock patterns for the comparable configurations probably occur behind the wing.

Drag characteristics.- As was found for the unswept-wing-body combination, the measured variation of the drag coefficient with Mach number for the delta-wing-body combination is the same as that for the comparable body of revolution within the probable accuracy of the measurements (fig. 5).

Swept Wing and Cylindrical Body

Shock phenomena.- Wall Mach number distributions indicate that, as was true for the unswept wing-body combination, the flow fields for the swept wing-body combination at a distance from the configuration are almost exactly the same as those for the comparable body of revolution.

The schlieren photographs of figure 6 and reference 5 indicate that near the speed of sound, the swept wing produces a weak shock at the trailing edge of the wing-body juncture and a strong shock behind the trailing edge of the juncture. At a Mach number of 1.03, an additional weak shock is also present between these two shocks. The losses in the two weak shocks are insignificant and may be neglected in a comparison of the total shock losses. The side-view schlieren photographs presented in figure 6 indicate that the main shock produced by the wing appears to be approximately the same as the shock caused by the comparable body in the region above the combination. However, the shock produced by the wing is generally somewhat rearward of that produced by the body. At a Mach number of 1.00, this shock for the wing is just visible in the schlieren photograph. Plan-view schlieren surveys not presented

herein indicate that near the wing tip the main shock produced by the wing is somewhat different from that caused by the comparable body, particularly at a Mach number of 1.10. (The shock in this region is similar to that for the same wing on the curved body (ref. 5).)

Drag characteristics.- The drag coefficient increments for the swept-wing and cylindrical-body combination are approximately 0.001 greater than those for the comparable body of revolution at Mach numbers up to approximately 1.02 (fig. 7). This difference is approximately the same as the total of the possible maximum errors of the drag measurements. However, assuming this discrepancy shown is real, it can logically be attributed to differences in the shock formations and associated boundary-layer separation. At higher Mach numbers, the differences between the drag increments for the comparable configurations increase primarily because of the more pronounced deviations of the shock formations. The greater differences between the drag-rise increments for this swept-wing-body combination and the comparable body of revolution in comparison with those for the unswept wing may be attributed primarily to the greater thickness ratio and smaller taper for the swept wing.

Swept Wing and Curved Body

Shock phenomena.- The shock formations as indicated in the schlieren side-view photograph for the swept-wing-curved-body combination (fig. 8) are similar to, but apparently stronger than, those for the swept-wing-cylindrical-body configuration (fig. 6). The differences between the shock formations produced by the swept-wing-curved-body configuration (fig. 8 and ref. 5) and those for the comparable body of revolution (fig. 8) are similar to the differences for the swept-wing-cylindrical-body combination.

Drag characteristics.- The combination of the swept wing and curved body results in a severe, adverse drag interference between the wing and body near the speed of sound. The drag-coefficient rise for the swept wing in combination with this body near the speed of sound is approximately 0.012 compared with a value of 0.004 for the wing in conjunction with the essentially interference-free cylindrical body (figs. 7 and 9). (These differences in the drag rise values may be due in part to the difference of the maximum body diameter as well as the large variation of the curvature of the afterbody.)

The pronounced drag-rise increments for the wing and curved body configuration are approximately 0.003 greater than those for the comparable body near the speed of sound (fig. 9). The maximum drag rise for the combination, as measured at a Mach number of 1.03, is approximately 15 percent greater than that for the comparable body of revolution.

These differences can be attributed to the same factors which caused the similar but smaller differences for the swept-wing-cylindrical body combination.

Of particular importance is the fact that the relative increase in the drag rise for the swept-wing—curved-body combination compared with that for the wing—cylindrical-body configuration is approximately the same as the relative increase for the comparable bodies of revolution.

Generalization

The results presented indicate that, near the speed of sound, the shock formations and the associated drag-rise characteristics for the various wing and central-body combinations investigated are, to the first order, the same as those for the bodies of revolution with the same axial distributions of cross-sectional area normal to the air stream. These bodies of revolution are simple axial developments of cross-sectional area. Therefore, on the basis of the results presented, it may logically be concluded that, near the speed of sound, the zero-lift drag rise of a thin low-aspect-ratio wing-body combination is primarily dependent on the axial distribution of cross-sectional areas normal to the air stream. It follows that the drag rise for any such configuration is approximately the same as that for any other with the same distribution of cross-sectional areas.

It may be assumed that this concept is also valid for wings alone, wings or wing-body combinations with moderate twist or camber, or yawed configurations; however, no directly comparable experimental results are available to substantiate these conjectures. Linear theory (ref. 9) and experiments (ref. 10) have indicated that a similar relation is valid for slender, noncircular bodies at supersonic, as well as at transonic speeds.

Applications of Transonic Drag-Rise Concept

Correlation of drag-rise characteristics.— The accuracy of a quantitative correlation of the drag rise of a conventional wing-body combination by using the proposed concept should be lessened by increasing the thickness ratio, aspect ratio, or taper ratio of the wing. The effects of enlarging these variables should become greater as the Mach number is increased beyond the speed of sound. The results presented herein indicate that usual variations of the shape of the body should have little effect on the accuracy of a quantitative correlation. The magnitudes of the section thickness ratios, aspect ratios, and taper ratios for the wings of contemporary transonic and supersonic aircraft generally lie between the values for the unswept and swept wings studies

herein. It may be assumed, therefore, that the accuracies of quantitative correlations of the drag-rise increments for these real configurations would be between those for the models investigated.

Because of the lack of knowledge as to the effects of detailed changes in the axial distributions of cross-sectional area on the drag-rise characteristics, quantitative correlations as presented herein are not generally feasible. However, it has been possible to correlate qualitatively all the available, reliable drag-rise results for wings and wing-body combinations (refs. 1, 2, 11, and 12, for example), by use of the available information for the effects of general changes in body shape on the transonic drag rise (refs. 7 and 13, for example). It appears that the concept should be generally useful in comparing the approximate relative effects of various design alterations.

A preliminary analysis of the available information defining the effects of nacelle position on the interference between the nacelle and the wing at transonic speeds (refs. 4 and 14, for example) indicated that this interference can be correlated qualitatively, at least, on the basis of the concept proposed. However, further specific experimental comparisons are required to define the exact applicability of this concept to the correlation of such interference.

An idea, similar to that proposed herein, was presented in reference 15 for predicting the critical speeds of wing-body combinations.

Interpretation of variations of drag-rise characteristics.- Analyses of the available drag-rise characteristics indicate that variations in wing configurations which result in less rapid rates of development of cross-sectional area, as well as reductions of the relative magnitude of the maximum areas, decrease the drag-rise increments near the speed of sound. For example, the rates of development and maximum value of the cross-sectional areas for the swept wing of the present investigation are less than those for the unswept wing (table II). As a result, the drag rise for the swept wing is less pronounced (figs. 3 and 7).

Reversing the unswept wing to form the delta wing (fig. 1) reduced the rate of expansion of cross-sectional area for the forward part of the wing, but increased the rate of contraction of area for the rearward part (table II). These variations resulted in increases of the drag-rise increments (figs. 3 and 5). On the basis of this comparison, as well as the results presented in reference 7, it may be assumed that, near the speed of sound, a given rate of decrease in cross-sectional area generally results in a greater drag rise than a similar increase.

On the basis of the proposed concept, adverse zero-lift drag interference between wings and bodies, as for the swept-wing-body combination

investigated (fig. 9), can generally be attributed basically to greater rates of development of the cross-sectional areas for the combinations compared with those for the components (table II). These more rapid variations of area generally result in higher induced velocities and considerably stronger shocks in the fields of the combinations. (For example, compare figs. 6 and 8.) Obviously the interference drags, associated with the increased shock losses, are directly produced by changes in the pressures on the body and wing. (For example, see ref. 5.) The favorable effects of various changes in body shape on the interference between the wing and body, as shown in references 2 and 12, can be attributed to reductions in the rates of development of the cross-sectional areas.

Reductions of the drag-rise increments of wing-body combinations.-

On the basis of the concept proposed, it would be expected that indenting the body of a wing-body combination, so that the combination has the same axial distribution of cross-sectional area as the original body alone, would result in a large reduction or elimination of the drag rise associated with the wing. The cylindrical body of figure 1, so indented, has been investigated in combination with the unswept, delta, and swept wings shown in figure 1.

As shown in figure 10, indenting the body reduced the drag-rise increments associated with the unswept and delta wings by approximately 60 percent near the speed of sound. This alteration eliminated the drag rise associated with the swept wing at Mach numbers up to 1.04. At higher Mach numbers, the effects of the indentations gradually decreased. Even for these relatively unconventional configurations, the proposed concept predicts correctly the qualitative effects of design modifications on the drag-rise characteristics near the speed of sound.

The incomplete effects of indenting the bodies with the unswept and delta wings may be attributed in part to the displacement of the stream tubes by the boundary layer, which was neglected in the design of the indentations. For the swept wing, this effect is less important because of the more gradual axial development of the wing. Minor modifications of the indentations of the body to account for this factor should further reduce the drag-rise increments associated with the unswept and delta wings. The reductions of the effects of these indentations at supersonic Mach numbers are associated with the change in the nature of the flow field at the higher speeds, as described in the discussion of the shock phenomena for the unswept wing.

At lift coefficients up to approximately 0.3, the indentations of the bodies result in drag reductions similar to those shown. While these indentations have not completely eliminated the near-sonic drag-rise increments associated with all the wings investigated, they have at least greatly reduced the increments in every case.

CONCLUSIONS

1. The shock phenomena and drag-rise increments measured for four representative wing and central-body combinations at zero lift near the speed of sound are essentially the same as those for bodies of revolution with the same axial distributions of cross-sectional areas normal to the air stream.

2. On the basis of these results, it is concluded that, near the speed of sound, the zero-lift drag rise of a thin, low-aspect-ratio wing-body combination is primarily dependent on the axial distribution of the cross-sectional areas normal to the air stream. It follows that the drag rise for any such configuration is approximately the same as that for any other with the same distribution of cross-sectional areas.

3. Indenting the bodies of three representative wing-body combinations, so that the axial distributions of cross-sectional areas for the combinations were the same as for the original body alone, greatly reduced or eliminated the zero-lift drag-rise increments associated with wings near the speed of sound.

Langley Aeronautical Laboratory
National Advisory Committee for Aeronautics
Langley Field, Va.

~~CONFIDENTIAL~~

REFERENCES

1. Bielat, Ralph P.: A Transonic Wind-Tunnel Investigation of the Aerodynamic Characteristics of Three 4-Percent-Thick Wings of Sweepback Angles 10.8° , 35° , and 47° , Aspect Ratio 3.5, and Taper Ratio 0.2 in Combination With a Body. NACA RM L52B08, 1952.
2. Langley Pilotless Aircraft Research Division: Some Recent Data From Flight Tests of Rocket-Powered Models. NACA RM L50K24, 1951.
3. Donlan, Charles J., Myers, Boyd C., II, and Mattson, Axel T.: A Comparison of the Aerodynamic Characteristics at Transonic Speeds of Four Wing-Fuselage Configurations as Determined From Different Test Techniques. NACA RM L50H02, 1950.
4. Pepper, William B., Jr., and Hoffman, Sherwood: Comparison of Zero-Lift Drags Determined by Flight Tests at Transonic Speeds of Symmetrically Mounted Nacelles in Various Spanwise Positions on a 45° Sweptback Wing and Body Combination. NACA RM L51D06, 1951.
5. Whitcomb, Richard T., and Kelly, Thomas C.: A Study of the Flow Over a 45° Sweptback Wing-Fuselage Combination at Transonic Mach Numbers. NACA RM L52D01, 1952.
6. Ritchie, Virgil S., and Pearson, Albin O.: Calibration of the Slotted Test Section of the Langley 8-Foot Transonic Tunnel and Preliminary Experimental Investigation of Boundary-Reflected Disturbances. NACA RM L51K14, 1952.
7. Thompson, Jim Rogers, and Kurbjun, Max C.: Drag Measurements at Transonic Speeds of Two Bodies of Fineness Ratio 9 With Different Locations of Maximum Body Diameter. NACA RM L8A28b, 1948.
8. Busemann, Adolf: Application of Transonic Similarity. NACA TN 2687, 1952.
9. Graham, Ernest W.: The Pressure on a Slender Body of Non-Uniform Cross-Sectional Shape in Axial Supersonic Flow. Rep. No. SM-13346-A, Douglas Aircraft Co., Inc., July 20, 1949.
10. Stoney, William E., Jr., and Putland, Leonard W.: Some Effects of Body Cross-Sectional Shape, Including a Sunken-Canopy Design, on Drag as Shown by Rocket-Powered-Model Tests at Mach Numbers From 0.8 to 1.5. NACA RM L52D07, 1952.

11. Nelson, Warren H., and McDevitt, John B.: The Transonic Characteristics of 17 Rectangular, Symmetrical Wing Models of Varying Aspect Ratio and Thickness. NACA RM A51A12, 1951.
12. Pepper, William B.: The Effect on Zero-Lift Drag of an Indented Fuselage or a Thickened Wing-Root Modification to a 45° Sweptback Wing-Body Configuration as Determined by Flight Tests at Transonic Speeds. NACA RM L51F15, 1951.
13. Thompson, Jim Rogers: Measurements of the Drag and Pressure Distribution on a Body of Revolution Throughout Transition From Subsonic to Supersonic Speeds. NACA RM L9J27, 1950.
14. Bielat, Ralph P., and Harrison, Daniel E.: A Transonic Wind-Tunnel Investigation of the Effects of Nacelle Shape and Position on the Aerodynamic Characteristics of Two 47° Sweptback Wing-Body Configurations. NACA RM L52G02, 1952.
15. Robinson, Russell G., and Wright, Ray H.: Estimation of Critical Speeds of Airfoils and Streamline Bodies. NACA ACR, Mar. 1940.

TABLE I
BASIC BODY ORDINATES

[All dimensions are in inches]

Cylindrical body	
Station	Radius
0	0
.225	.104
.338	.134
.563	.193
1.125	.325
2.250	.542
3.375	.726
4.500	.887
6.750	1.167
9.000	1.391
11.250	1.559
13.500	1.683
15.750	1.770
18.000	1.828
20.250	1.864
22.500	1.875
43.000	1.875

Curved body	
Station	Radius
0	0
.200	.092
.300	.119
.500	.171
1.000	.289
2.000	.482
3.000	.645
4.000	.788
6.000	1.037
8.000	1.236
10.000	1.386
12.000	1.496
14.000	1.573
16.000	1.625
18.000	1.657
20.000	1.667
22.000	1.652
24.000	1.610
26.000	1.537
28.000	1.425
30.000	1.251
32.000	1.010
32.605	0.940



TABLE II
ORDINATES OF REVISED BODIES OF REVOLUTION

[All dimensions are in inches]

Comparable to unswept wing on cylindrical body	
Station	Radius
22.500	1.875
23.500	1.875
24.500	1.892
25.000	1.939
25.500	2.012
26.000	2.087
26.500	2.155
27.000	2.182
27.500	2.185
28.000	2.174
28.500	2.145
29.000	2.113
29.500	2.086
30.000	2.054
30.500	2.019
31.000	1.992
31.500	1.968
32.000	1.934
32.500	1.911
33.000	1.894
33.500	1.882
34.000	1.875
43.000	1.875

Comparable to delta wing on cylindrical body	
Station	Radius
22.500	1.875
24.000	1.875
24.500	1.882
25.000	1.894
25.500	1.911
26.000	1.934
26.500	1.968
27.000	1.992
27.500	2.019
28.000	2.054
28.500	2.086
29.000	2.113
29.500	2.145
30.000	2.174
30.500	2.185
31.000	2.182
31.500	2.155
32.000	2.087
32.500	2.012
33.000	1.939
33.500	1.892
34.500	1.875
43.000	1.875



TABLE II - Concluded
ORDINATES OF REVISED BODIES OF REVOLUTION

[All dimensions are in inches]

Comparable to swept wing on cylindrical body	
Station	Radius
22.500	1.875
23.125	1.875
24.125	1.907
25.125	1.957
26.125	2.024
27.125	2.080
28.125	2.117
29.125	2.143
30.125	2.135
31.125	2.107
32.125	2.083
33.125	2.071
34.125	2.045
35.125	2.001
36.125	1.946
37.125	1.899
38.125	1.876
38.375	1.875
43.000	1.875

Comparable to swept wing on curved body	
Station	Radius
14.000	1.573
14.300	1.580
14.625	1.595
15.625	1.670
16.625	1.747
17.625	1.836
18.625	1.903
19.625	1.943
20.625	1.966
21.625	1.949
22.625	1.901
23.625	1.857
24.625	1.822
25.625	1.756
26.625	1.664
27.625	1.545
28.625	1.413
29.625	1.292
29.875	1.260
30.000	1.251
32.000	1.010
32.605	0.940



TABLE III
ORDINATES OF INDENTED BODIES

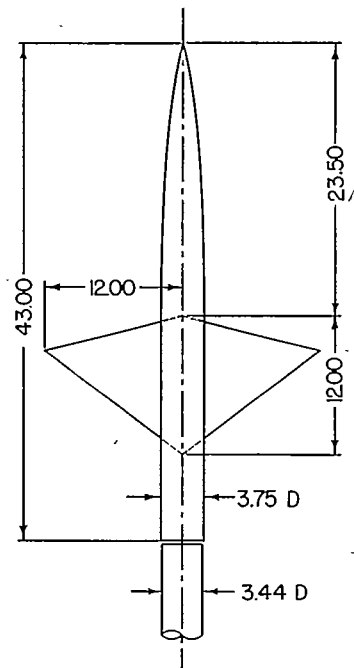
[All dimensions are in inches]

With unswept wing	
Station	Radius
22.500	1.875
24.000	1.875
24.500	1.857
25.000	1.807
25.500	1.720
26.000	1.622
26.500	1.521
27.000	1.476
27.500	1.470
28.000	1.487
28.500	1.533
29.000	1.580
29.500	1.642
30.000	1.664
30.500	1.710
31.000	1.743
31.500	1.773
32.000	1.812
32.500	1.837
33.000	1.856
33.500	1.868
34.000	1.875
43.000	1.875

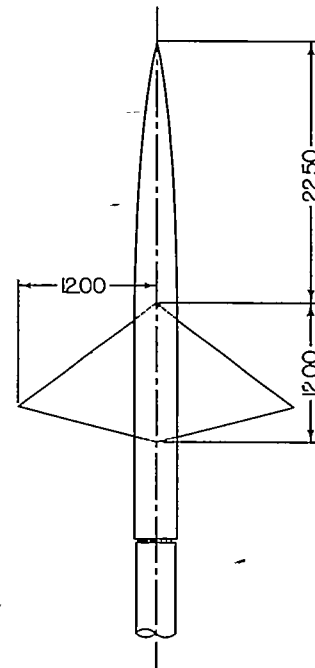
With delta wing	
Station	Radius
22.500	1.875
24.000	1.875
24.500	1.868
25.000	1.856
25.500	1.837
26.000	1.812
26.500	1.773
27.000	1.743
27.500	1.710
28.000	1.664
28.500	1.642
29.000	1.580
29.500	1.533
30.000	1.487
30.500	1.470
31.000	1.476
31.500	1.521
32.000	1.622
32.500	1.720
33.000	1.807
33.500	1.857
34.000	1.875
43.000	1.875

With swept wing	
Station	Radius
22.500	1.875
23.125	1.875
24.125	1.842
25.125	1.787
26.125	1.710
27.125	1.641
28.125	1.592
29.125	1.560
30.125	1.572
31.125	1.611
32.125	1.640
33.125	1.656
34.125	1.688
35.125	1.740
36.125	1.802
37.125	1.850
38.125	1.874
38.375	1.875
43.000	1.875

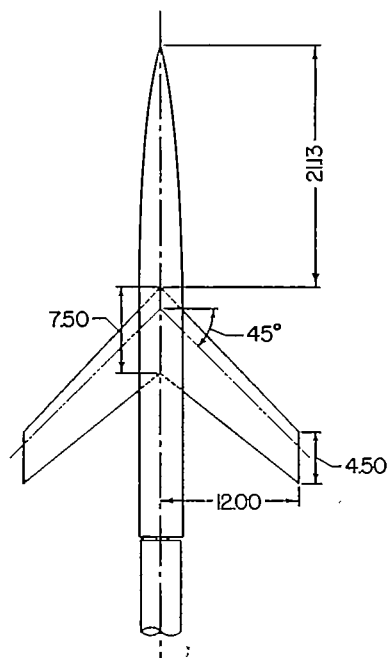




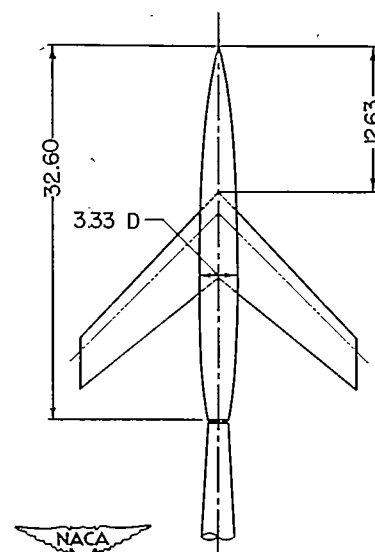
(a) Unswept wing, cylindrical body.



(b) Delta wing, cylindrical body.

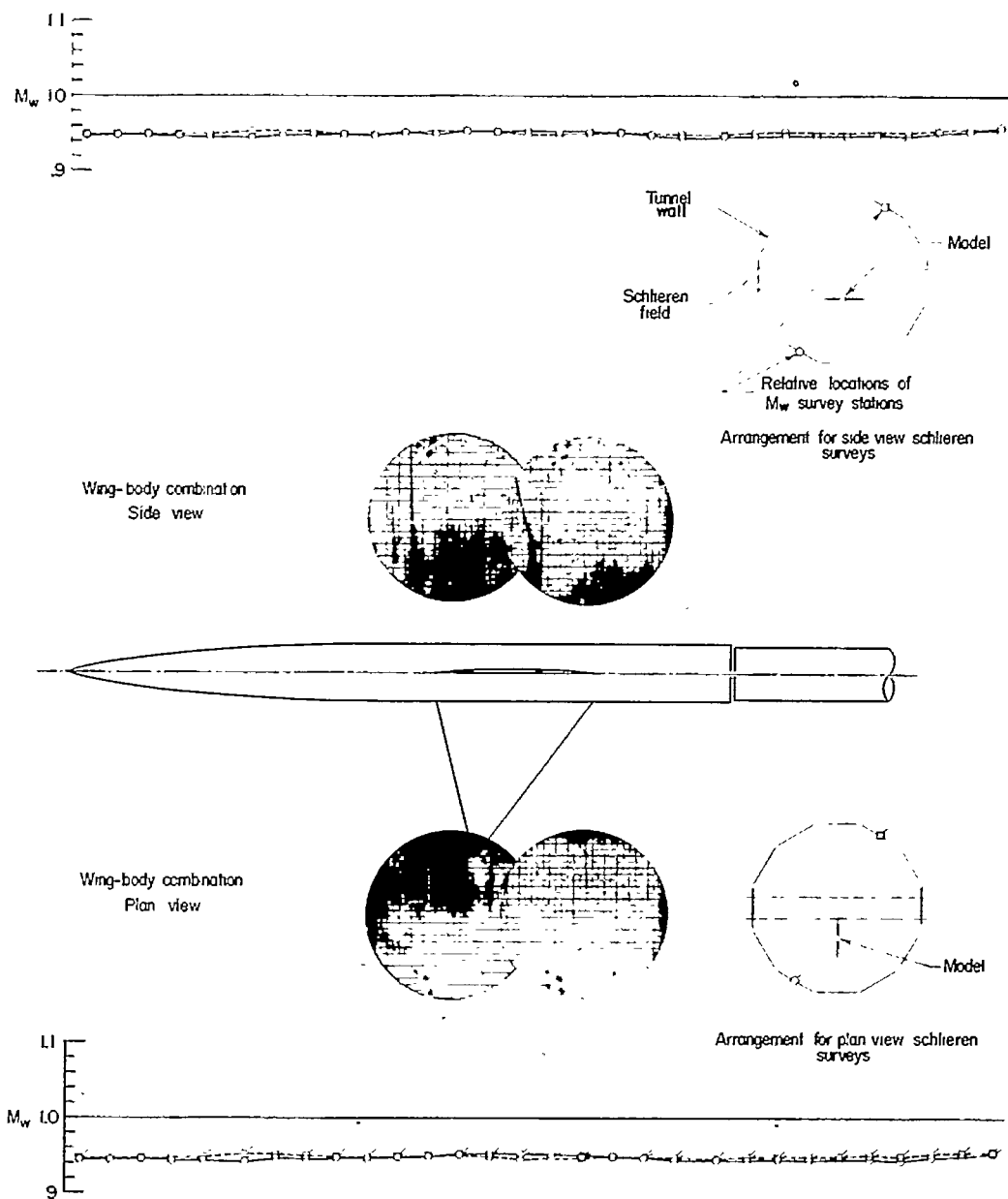


(c) Swept wing, cylindrical body.



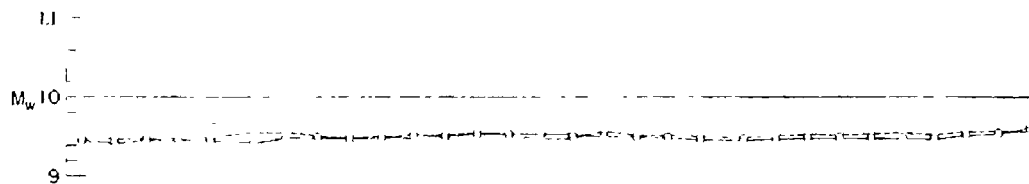
(d) Swept wing, curved body.

Figure 1.- Wing-body combinations used in investigation. All dimensions are in inches.

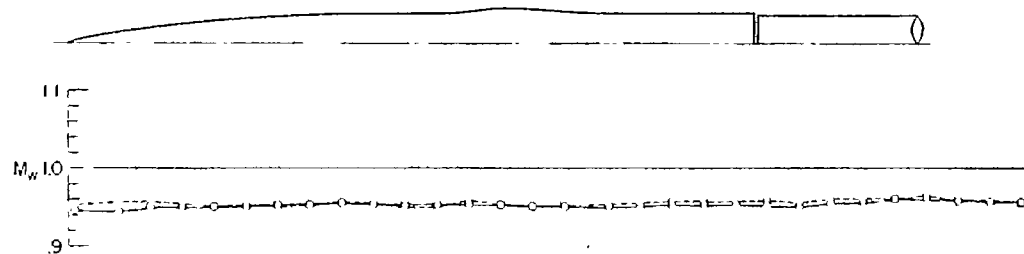
(a) $M_0 = 0.95$.

NACA
L-76100

Figure 2.- Comparisons of the shock phenomena for the unswept-wing and cylindrical-body combination with those for the comparable body of revolution and the cylindrical body alone.



Comparable body of revolution
Side view



Cylindrical body
Side view

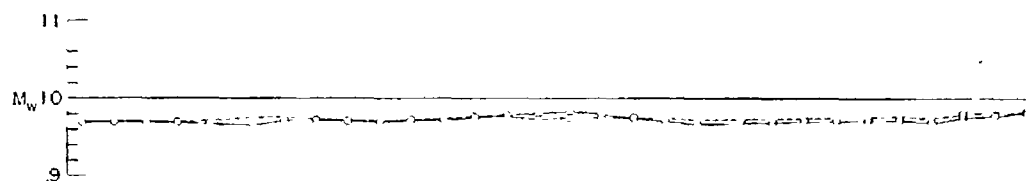
(a) $M_0 = 0.95$. Concluded.

NACA
L-76101.1

Figure 2.- Continued.

~~CONFIDENTIAL~~

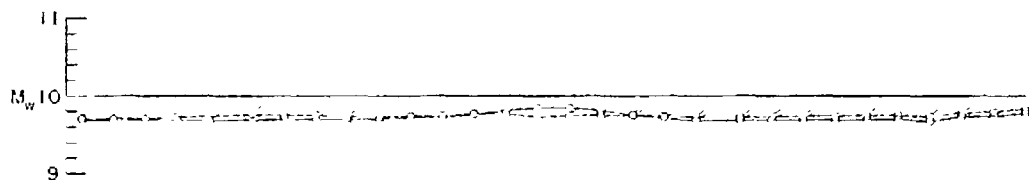
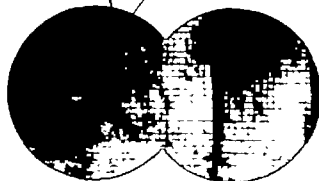
NACA RM L52H08



Wing-body combination
Side view



Wing-body combination
Plan view

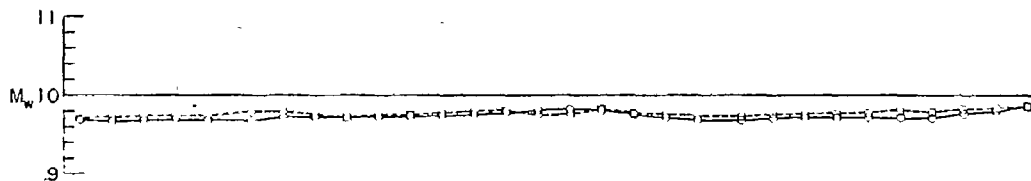


(b) $M_o = 0.98$. See figure 2(a)
for test-point arrangement.

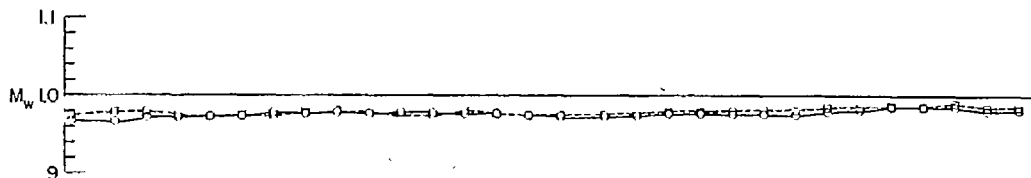
Figure 2.- Continued.

NACA
L-76102

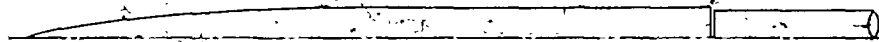
~~CONFIDENTIAL~~



Comparable body of revolution
Side view



Cylindrical body
Side view



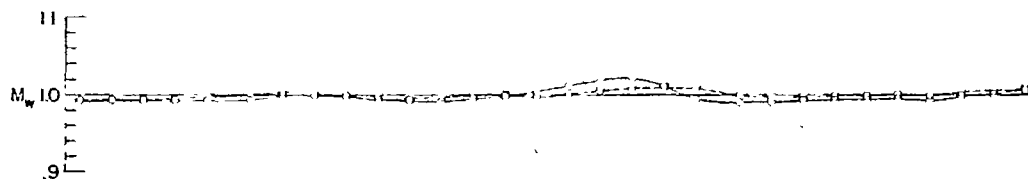
(b) $M_o = 0.98$. Concluded.

Figure 2.- Continued.

NACA
L-76103

~~CONFIDENTIAL~~

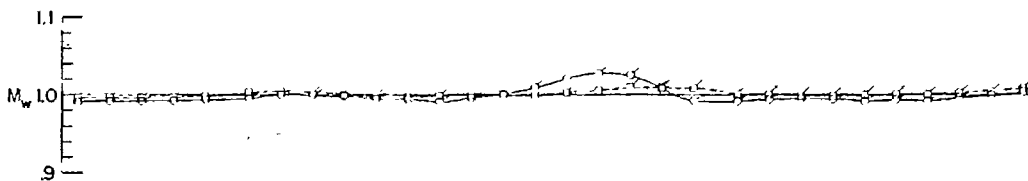
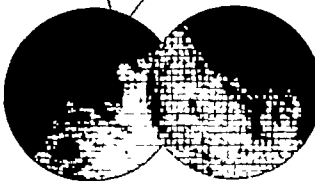
NACA RM L52H08



Wing-body combination
Side view



Wing-body combination
Plan view

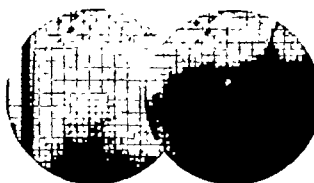
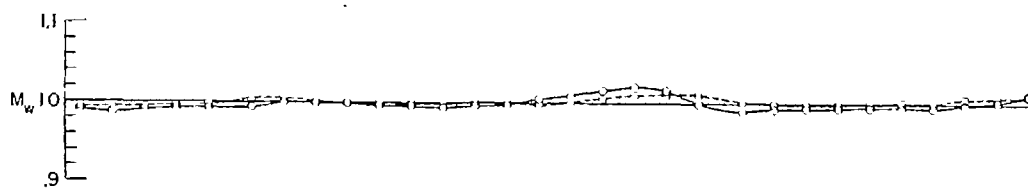


(c) $M_o = 1.00$. See figure 2(a)
for test-point arrangement.

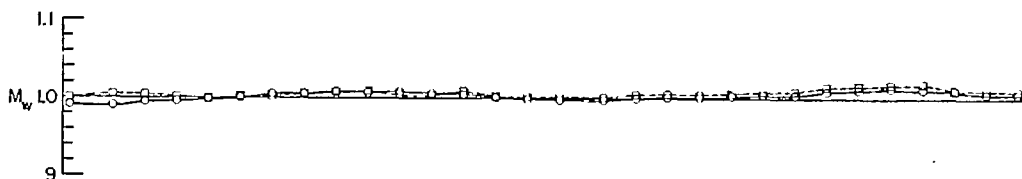
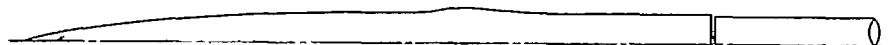
NACA
L-76104

Figure 2.- Continued.

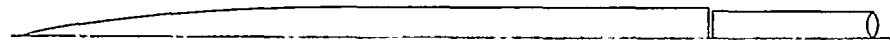
~~CONFIDENTIAL~~

~~CONFIDENTIAL~~

Comparable body of revolution
Side view



Cylindrical body
Side view



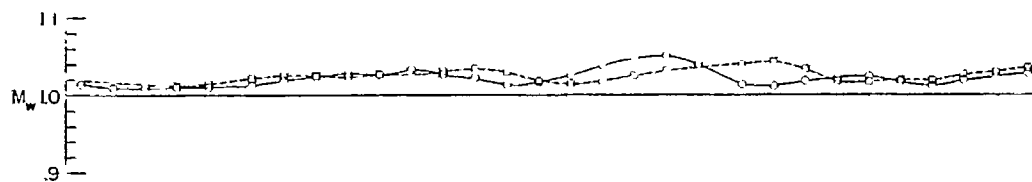
(c) $M_o = 1.00$. Concluded.

Figure 2.- Continued.

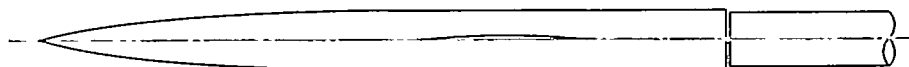
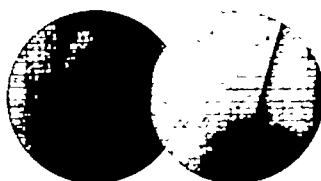


L-76105

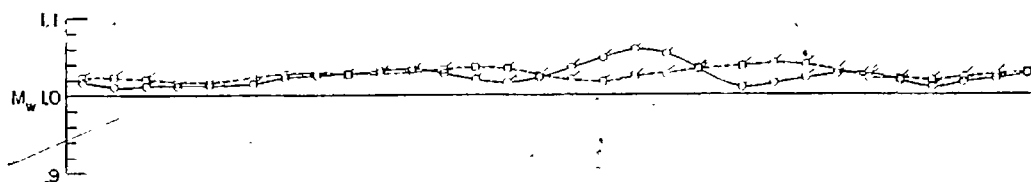
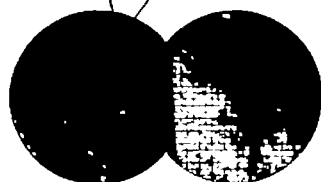
~~CONFIDENTIAL~~



Wing-body combination
Side view



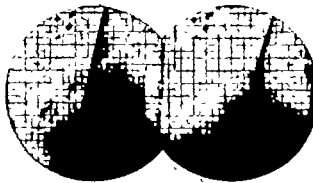
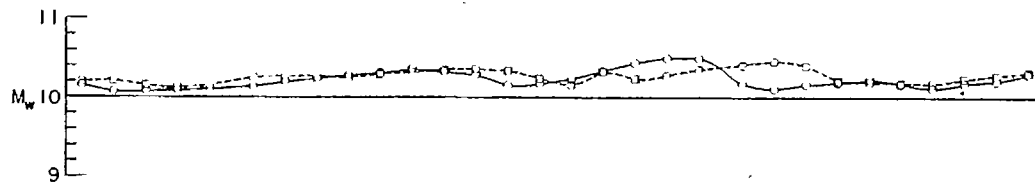
Wing-body combination
Plan view



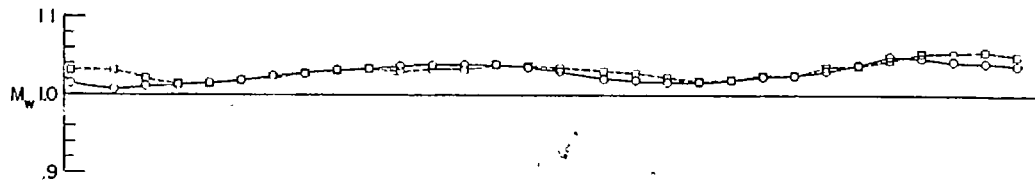
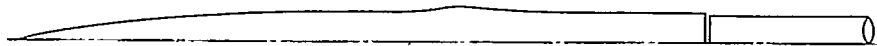
(d) $M_0 = 1.03$. See figure 2(a)
for test-point arrangement.

Figure 2.- Continued.

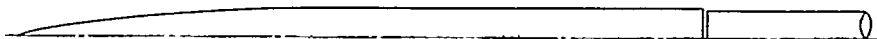
NACA
L-76106



Comparable body of revolution
Side view



Cylindrical body
Side view



(d) $M_0 = 1.03$. Concluded.

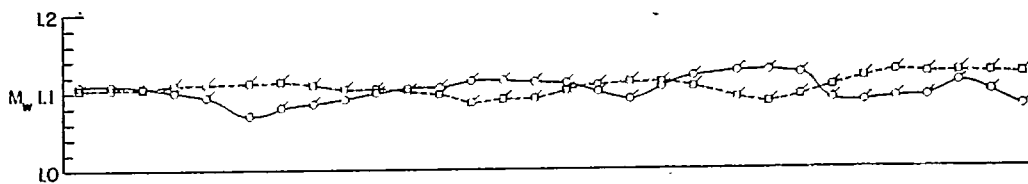
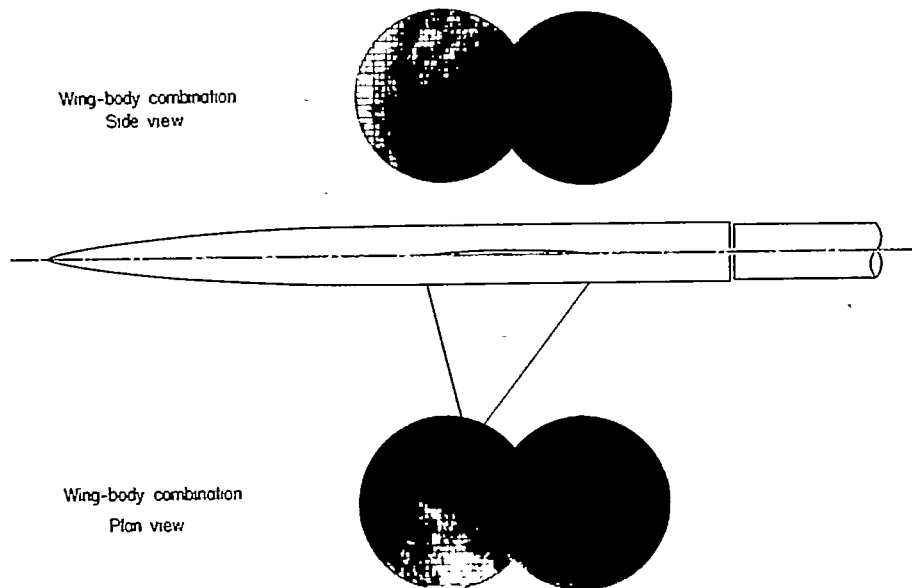
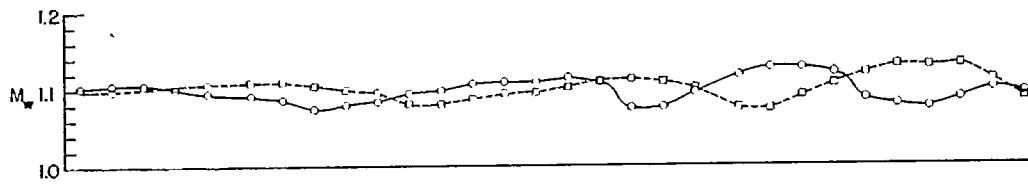
Figure 2.- Continued.



L-76107

~~CONFIDENTIAL~~

NACA RM L52H08

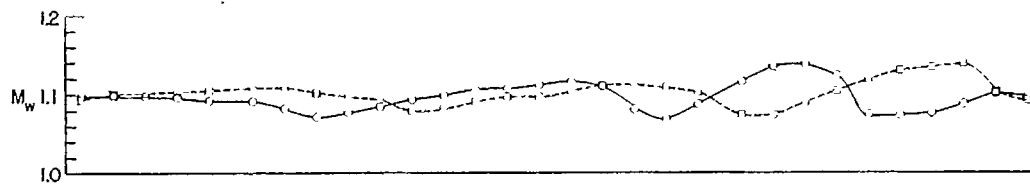


(e) $M_o = 1.10$. See figure 2(a)
for test-point arrangement.

Figure 2.- Continued.

NACA
L-76108

~~CONFIDENTIAL~~

~~CONFIDENTIAL~~

a

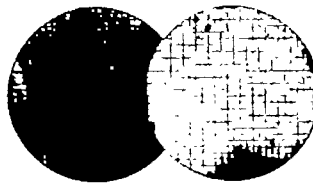
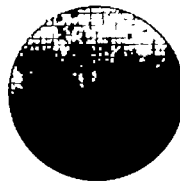
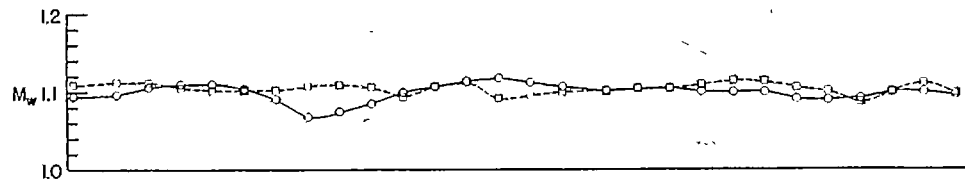
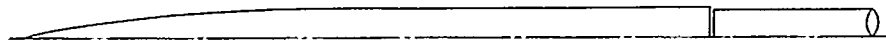
Comparable body of revolution
Side viewCylindrical body
Side view(e) $M_o = 1.10$. Concluded.

Figure 2.- Concluded.



L-76109

~~CONFIDENTIAL~~

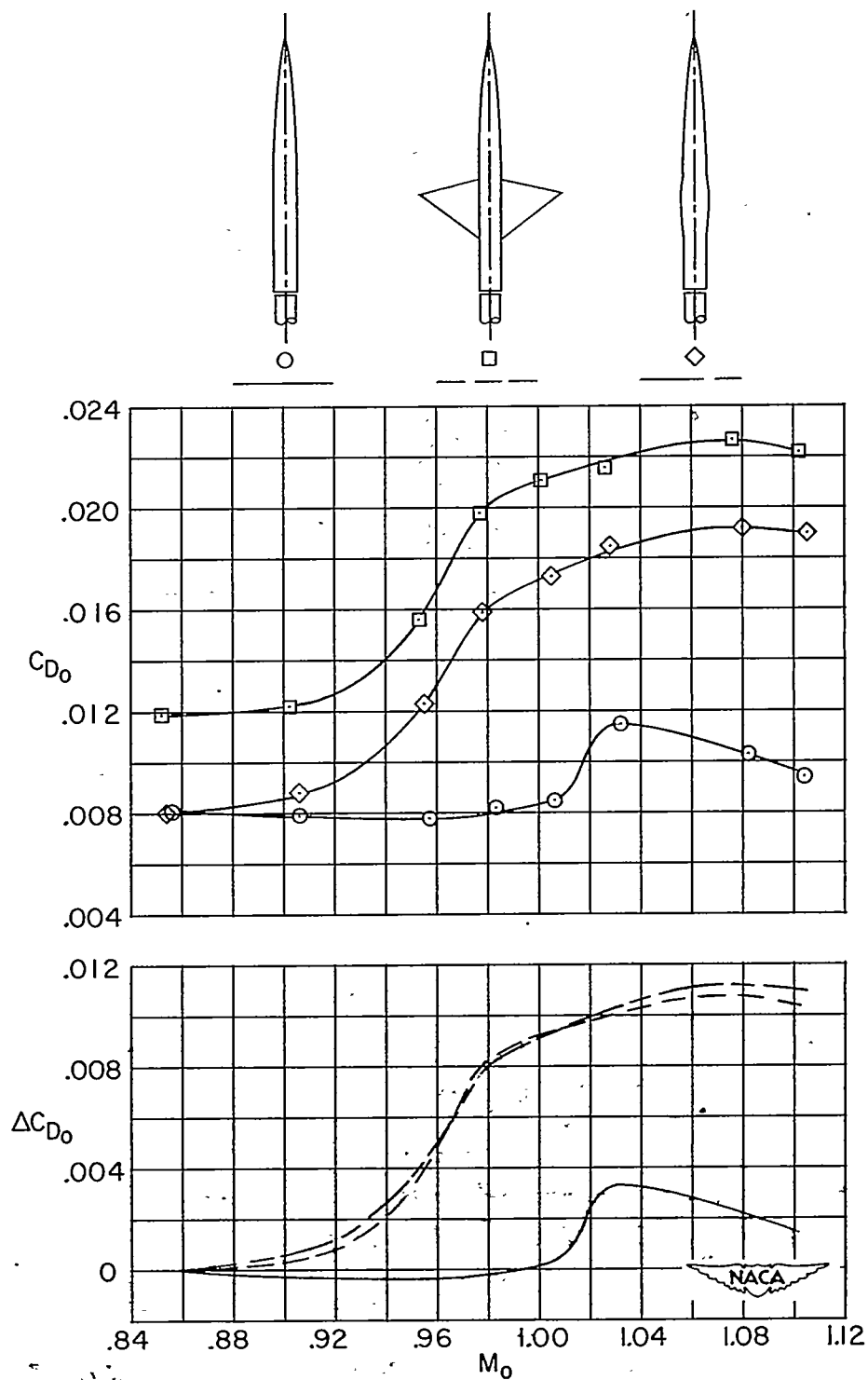
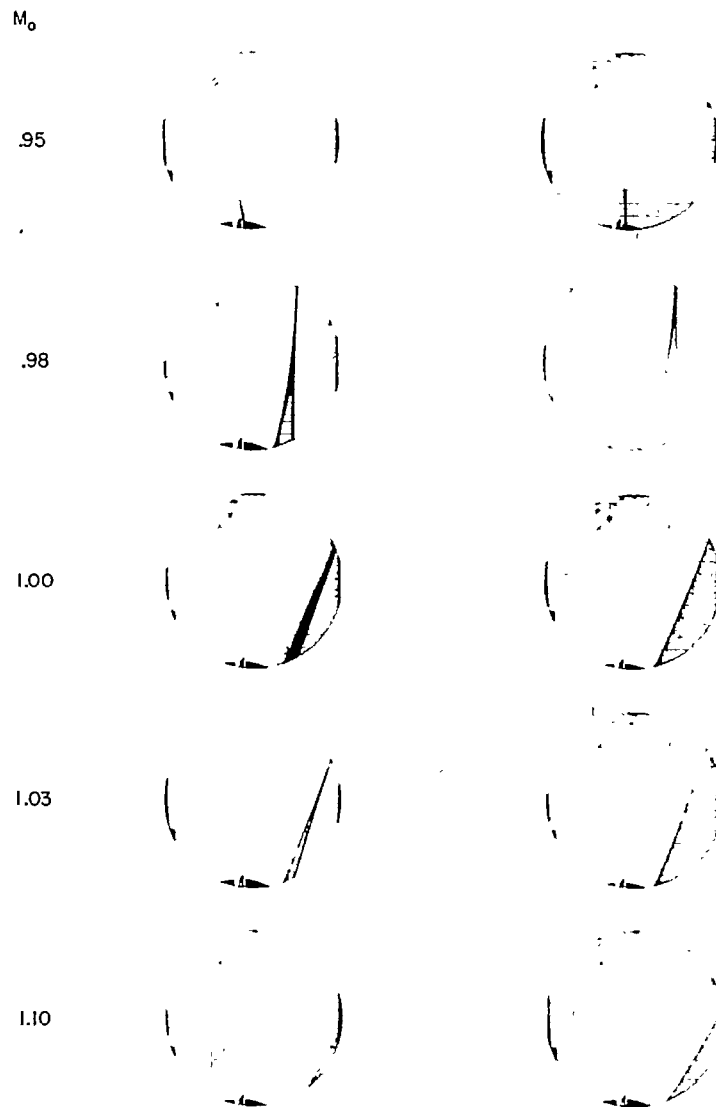


Figure 3.- Comparisons of the drag rise for the unswept-wing and cylindrical-body combination with that for the comparable body of revolution and the cylindrical body alone.



NACA

NACA

L-76110

Figure 4.- Comparisons of the shock phenomena for the delta-wing and cylindrical-body combination with those for the comparable body of revolution. Side views.

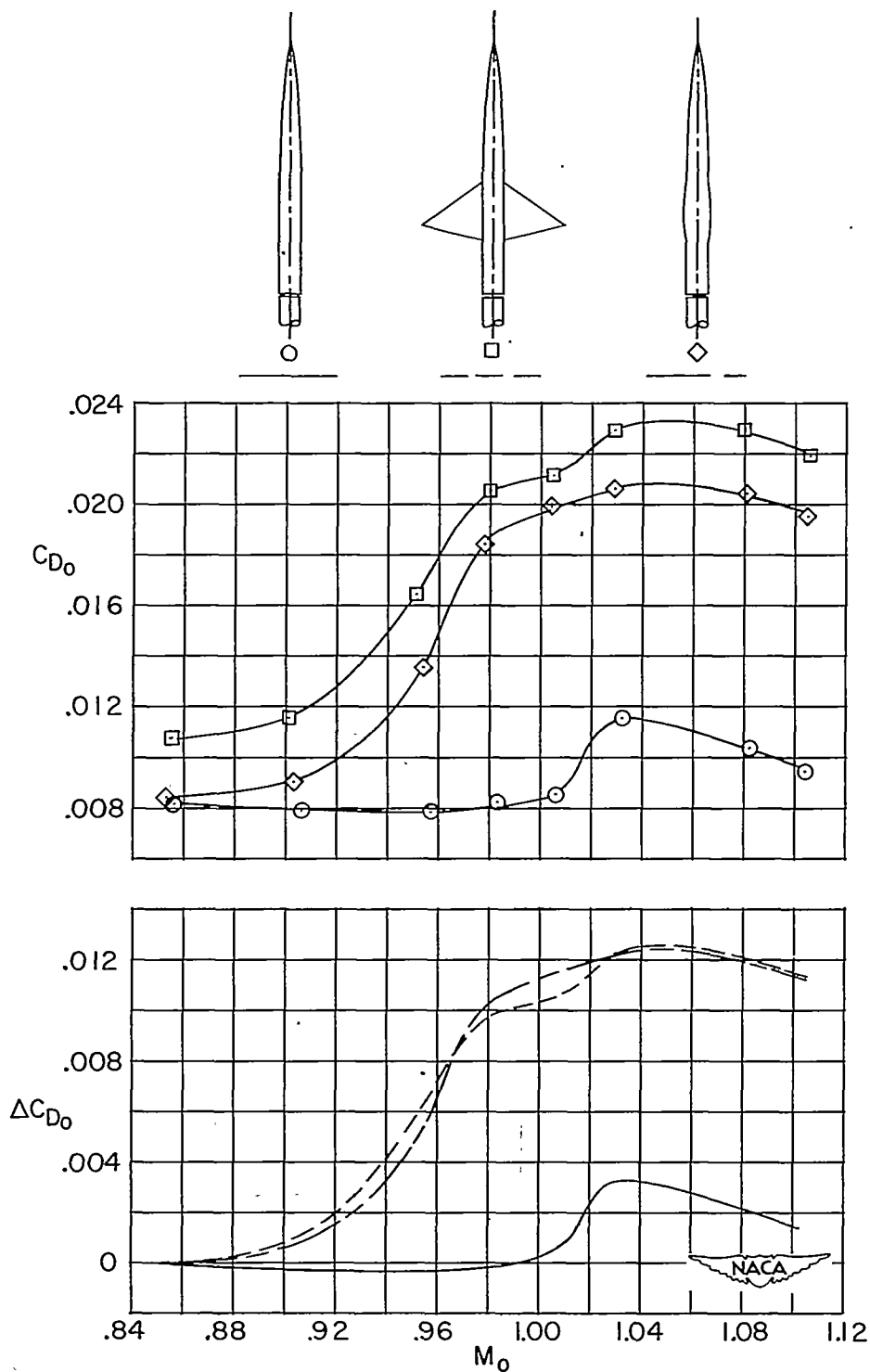
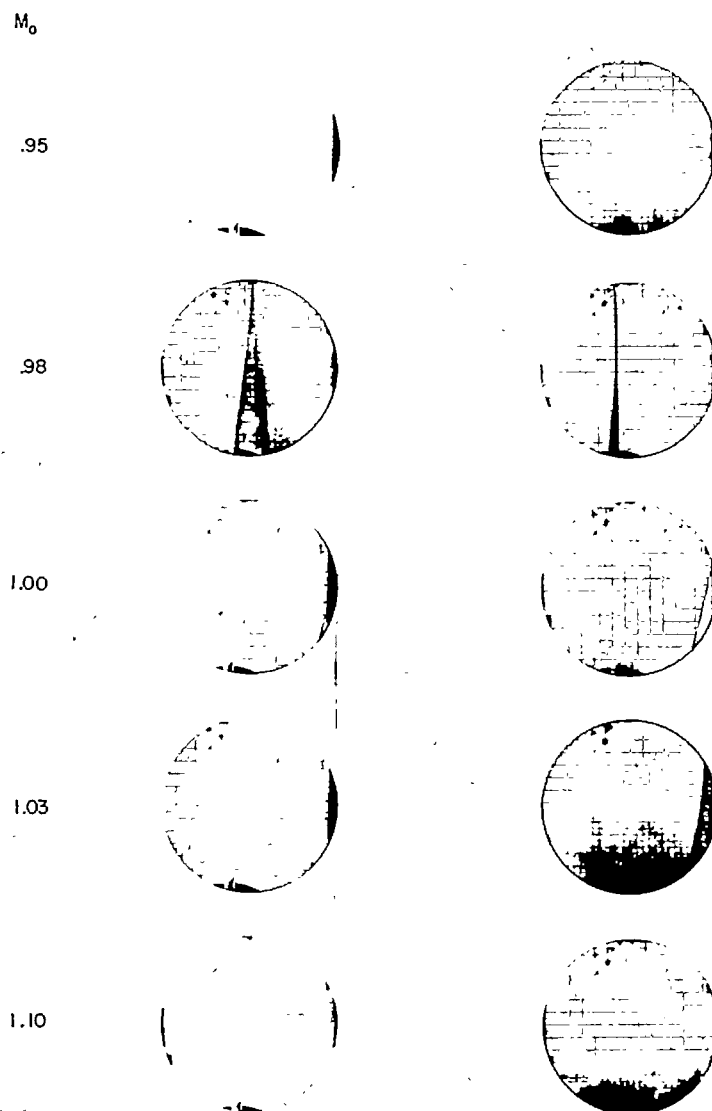
~~CONFIDENTIAL~~

Figure 5.- Comparisons of the drag rise for the delta-wing and cylindrical-body combination with that for the comparable body of revolution and the cylindrical body alone.

~~CONFIDENTIAL~~



NACA

L-76111

Figure 6.- Comparisons of the shock phenomena for the swept-wing and cylindrical-body combination with those for the comparable body of revolution. Side views.

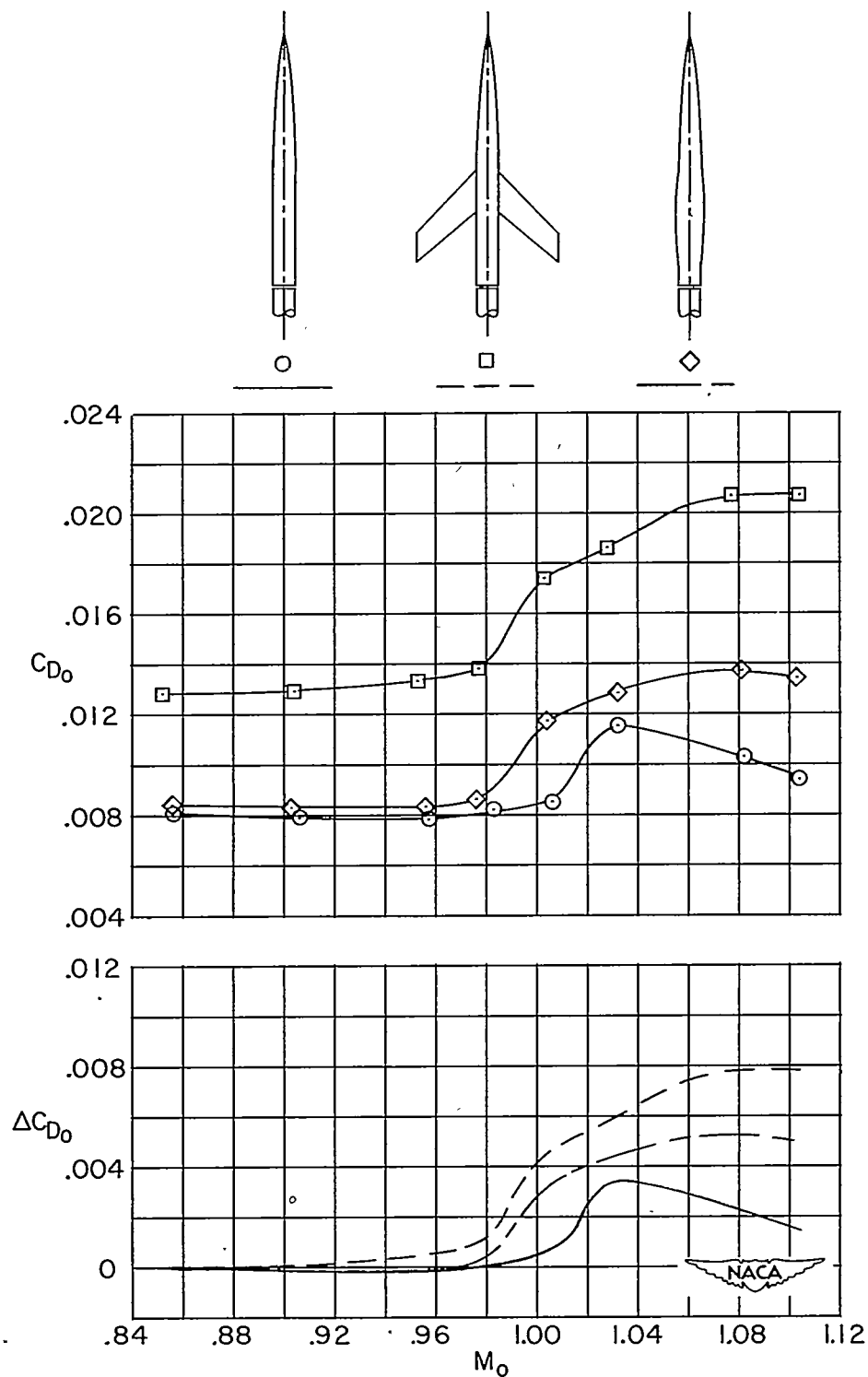
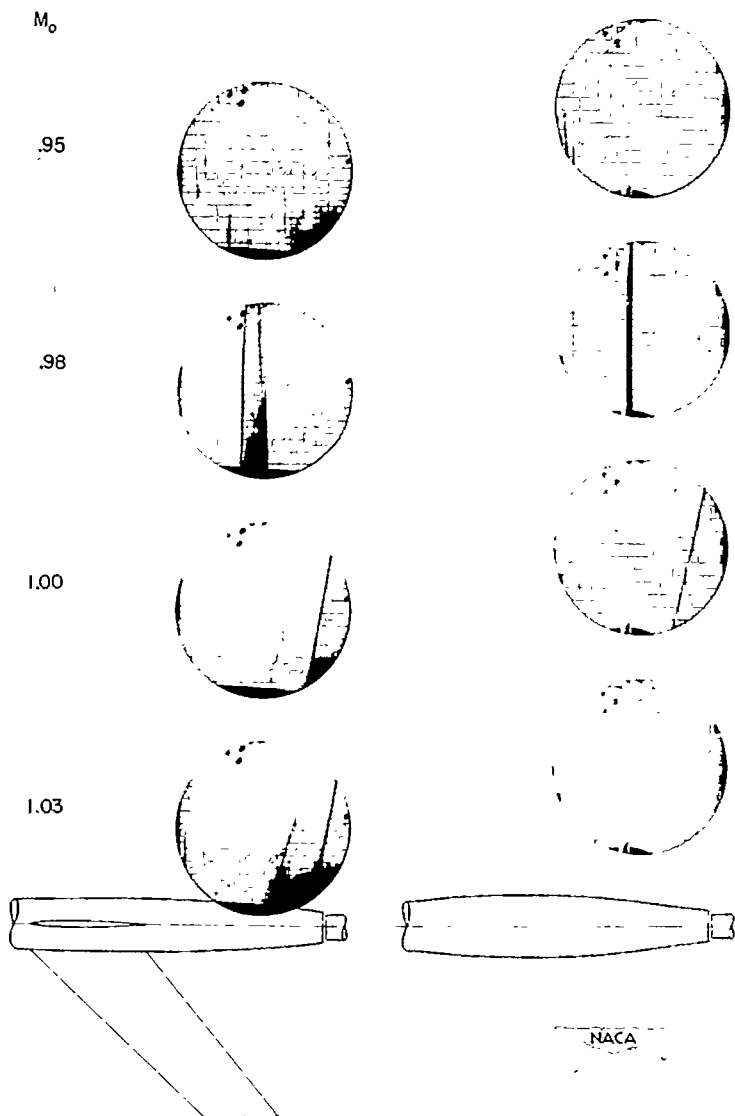


Figure 7.- Comparisons of the drag rise for the swept-wing and cylindrical-body combination with that for the comparable body of revolution and the cylindrical body alone.



NACA
L-76112

Figure 8.- Comparisons of the shock phenomena for the swept-wing and curved-body combination with those for the comparable body of revolution. Side views.

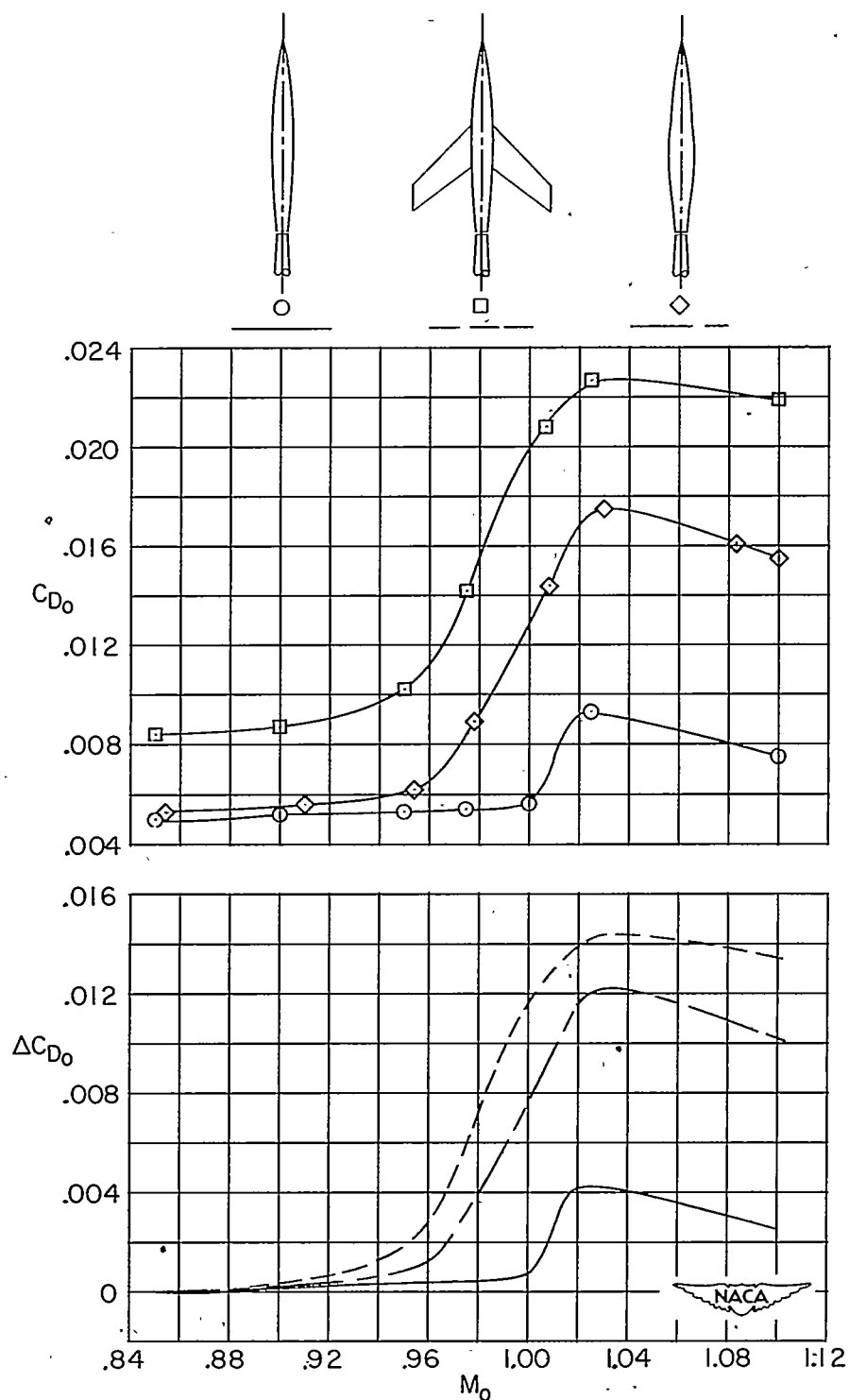
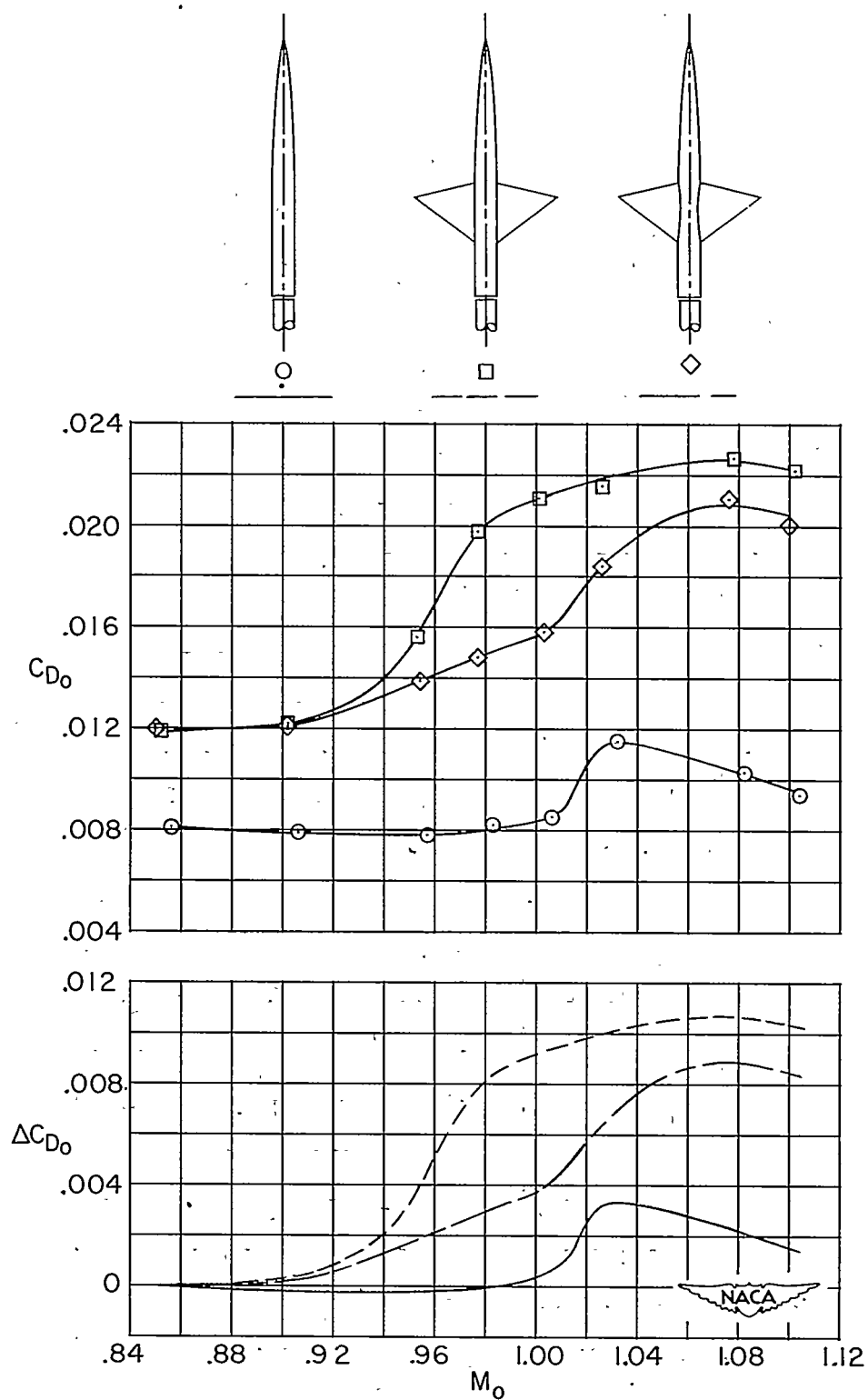
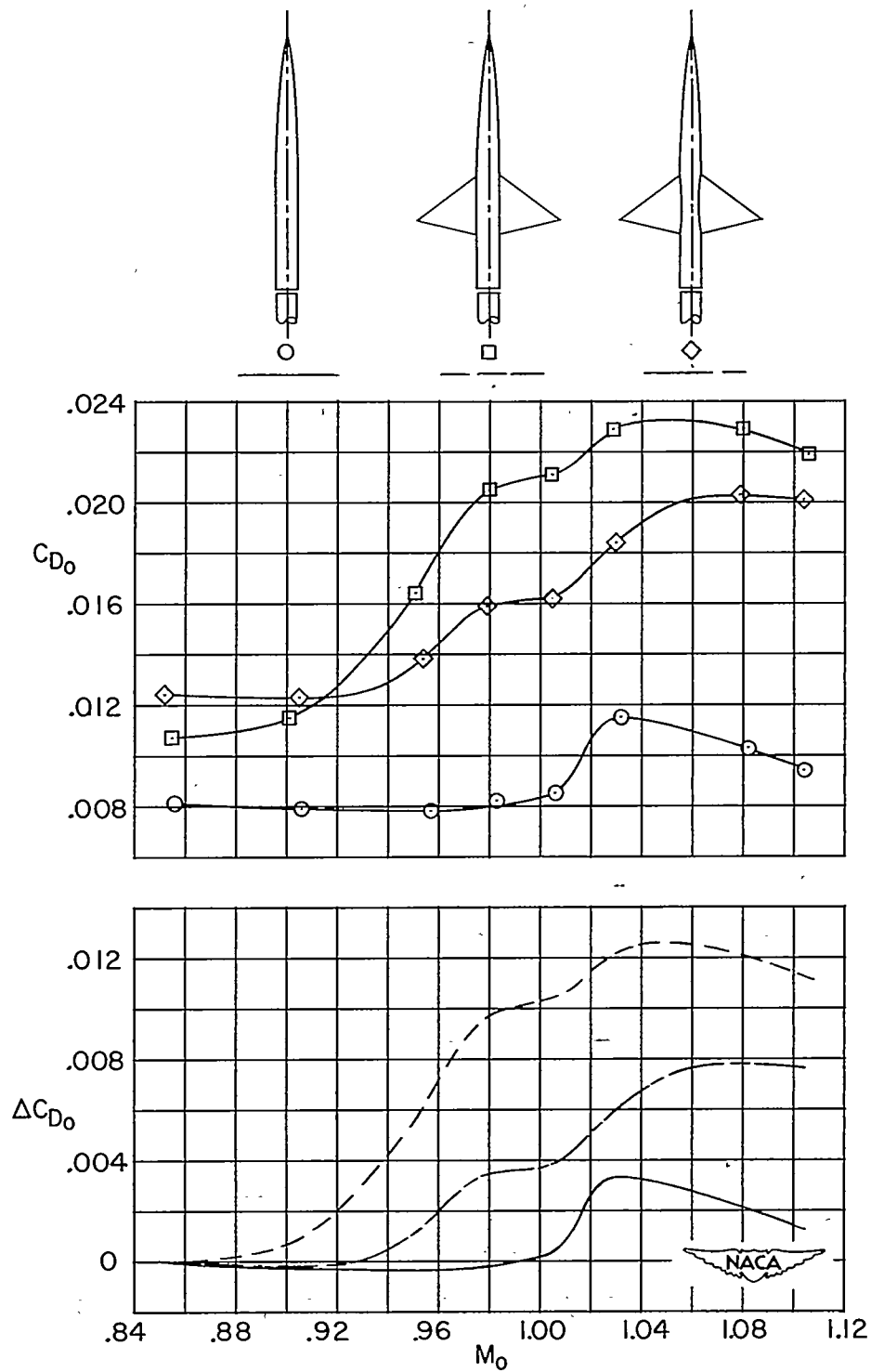


Figure 9.- Comparisons of the drag rise for the swept-wing and curved-body combination with that for the comparable body of revolution and the curved body alone.



(a) Unswept wing.

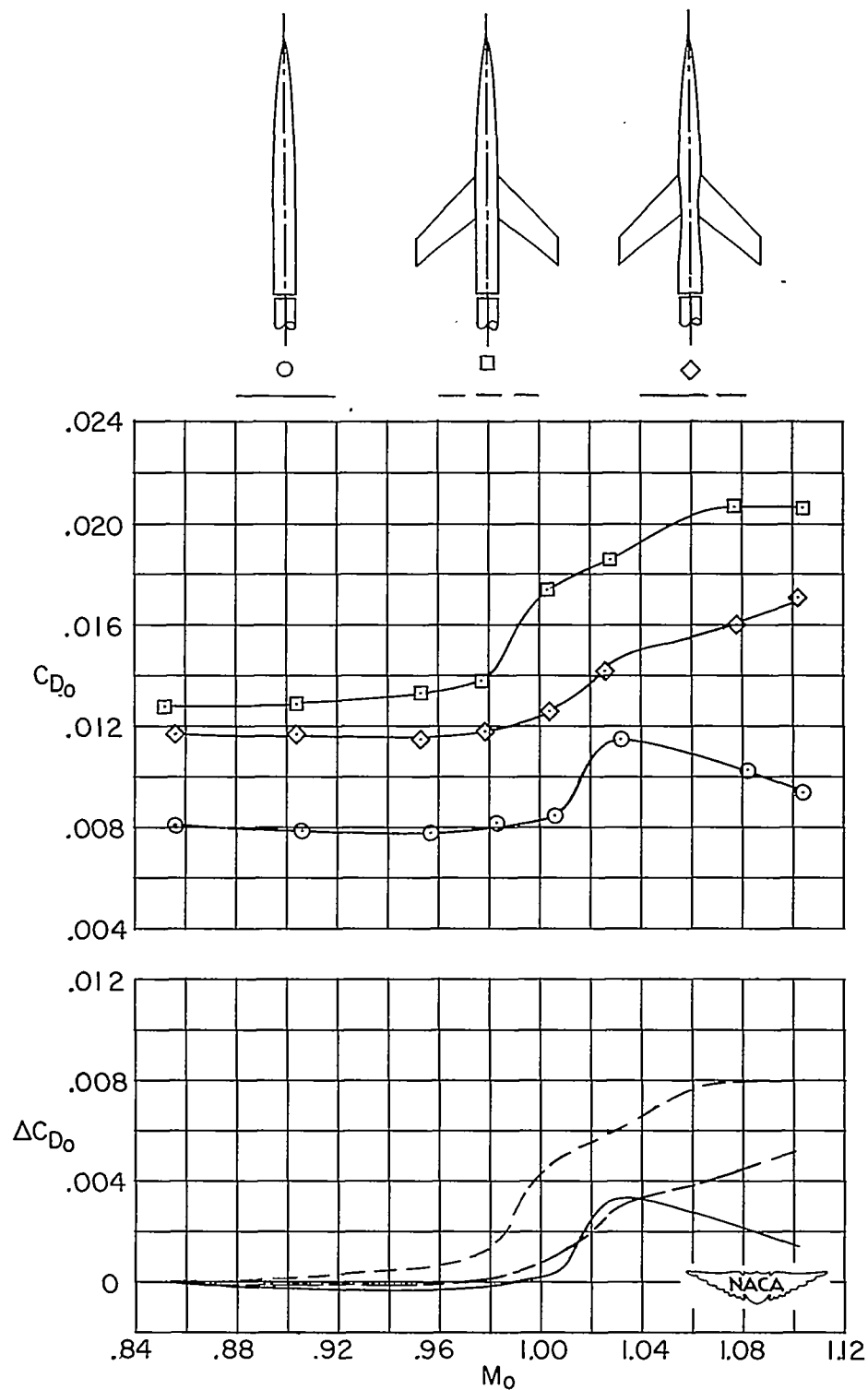
Figure 10.- The effects on transonic drag obtained by indenting the bodies of three wing-body combinations.

~~CONFIDENTIAL~~

(b) Delta wing.

Figure 10.- Continued.

~~CONFIDENTIAL~~



(c) Swept wing.

Figure 10.- Concluded.